African Journal of Advanced Pure and Applied Sciences (AJAPAS)
*Online ISSN: 2957-644X*
Volume 4, Issue 2, April - June 2025
Page No: 12-20
Website: https://aaasjournals.com/index.php/ajapas/index
ISI 2024: 0.877 SJIFactor 2024: 6.752 معامل التأثير العربي: 1.62

# The Effect of the Ionosphere on Ground-to-Satellite Communication Signals

Marai M. Abousetta [1], Ahdoud M. Issa [2*]
[1,2] Department of Electrical and Computer Engineering, Libyan Academy, Tripoli, Libya

# تأثير طبقة الأيونوسفير على إشارات الاتصالات بين الأرض والأقمار الصناعية

مرعي محمد أبوستة [1]، احدود ميلاد بوقنيدة [2*]
[2،1] قسم الهندسة الكهربائية والحاسوب، الأكاديمية الليبية، طرابلس، ليبيا

[*]Corresponding author: ehdod.m.e1980@gmail.com

| Received: January 25, 2025 | Accepted: March 23, 2025 | Published: April 05, 2025 |
|---|---|---|

**Abstract :**
The ionosphere is a dynamic plasma layer in Earth's upper atmosphere that significantly influences communication between ground stations and satellites. This study investigates the interaction of electromagnetic waves with ionospheric plasma, focusing on key parameters affecting plasma properties and signal propagation. Using the Finite-Difference Time-Domain (FDTD) method, simulations were conducted to analyze wave propagation, absorption, and dispersion through the ionosphere. Results indicate that Total Electron Content (TEC) decreases with increasing microwave frequency. Higher-frequency waves exhibit greater transmission coefficients, enabling penetration through the ionosphere, whereas lower-frequency signals experience significant attenuation—particularly in the D-layer during daylight hours. Effective collision frequency diminishes with altitude due to reduced atmospheric density, directly impacting signal reflection and absorption. TEC peaks at midday due to solar ionization and declines nocturnally, consistent with electron density fluctuations in the ionospheric layers. Analyses of group delay and frequency effects further reveal time-dependent signal propagation characteristics. These findings are critical for optimizing satellite communication, navigation systems, and remote sensing technologies reliant on microwave transmission through the ionosphere.

**Keywords**: Transmission coefficient, Signal penetration, Effective collision frequency, Collisions, Atmospheric density, Total electron content (TEC).

**الملخص**
الأيونوسفير هو طبقة بلازما ديناميكية في الغلاف الجوي العلوي للأرض تؤثر بشكل كبير على الاتصالات بين المحطات الأرضية والأقمار الصناعية. تبحث هذه الدراسة في تفاعل الموجات الكهرومغناطيسية مع بلازما الأيونوسفير، مع التركيز على المعلمات الرئيسية التي تؤثر على خصائص البلازما وانتشار الإشارة. باستخدام طريقة مجال الوقت ذي الفرق المحدود (FDTD)، أجريت عمليات محاكاة لتحليل انتشار الموجات والامتصاص والتشتت عبر الأيونوسفير. تشير النتائج إلى أن المحتوى الكلي للإلكترون (TEC) يتناقص مع زيادة تردد الموجات الدقيقة. تُظهر الموجات ذات التردد الأعلى معاملات انتقال أكبر، مما يتيح الاختراق عبر الأيونوسفير، بينما تعاني الإشارات ذات التردد المنخفض من التوهين الكبير - لا سيما في طبقة D خلال ساعات النهار. ينخفض تردد الاصطدام الفعال مع الارتفاع بسبب انخفاض كثافة الغلاف الجوي، مما يؤثر بشكل مباشر على انعكاس الإشارة وامتصاصها. يبلغ المحتوى الكلي للإلكترون ذروته في منتصف النهار بسبب التأين الشمسي وينخفض ليلاً، بما يتفق مع تقلبات كثافة الإلكترون في طبقات الأيونوسفير. تكشف تحليلات تأخير المجموعة وتأثيرات التردد عن خصائص انتشار الإشارة المعتمدة على الزمن. تُعد هذه النتائج بالغة الأهمية لتحسين الاتصالات عبر الأقمار الصناعية، وأنظمة الملاحة، وتقنيات الاستشعار عن بُعد المعتمدة على انتقال الموجات الدقيقة عبر طبقة الأيونوسفير.

**الكلمات المفتاحية**: معامل الإرسال، اختراق الإشارة، تردد التصادم الفعال، التصادمات، الكثافة الجوية، المحتوى الإلكتروني الكلي (TEC).

## I. Introduction

The ionosphere is a layer of ionized gas in Earth's upper atmosphere, spanning altitudes of approximately 60 km to 1000 km. In this region, solar ultraviolet radiation ionize gases, creating a dynamic plasma of free electrons and ions. This plasma interacts with electromagnetic (EM) waves, influencing wireless communications, navigation systems, and space weather phenomena [1]. Structurally, the ionosphere comprises four primary layers. The D-layer, the lowest region (60–90 km), exists only during daylight hours and weakly absorbs high-frequency signals. Above it, the E-layer (90–160 km) reflects radio waves, enabling long-distance terrestrial communication [2]. Studying EM wave propagation in the ionosphere is critical for satellite and radio communications. The ionosphere's ability to reflect and refract EM waves facilitates over-the-horizon signal transmission, but its dynamic nature—influenced by solar activity, geomagnetic storms, and high-power microwave pulses—poses challenges for signal reliability [7]. Key parameters governing ionospheric behavior include plasma frequency (the natural oscillation frequency of electrons in plasma), cyclotron frequency (electron gyration in Earth's magnetic field), and collision frequency (electron-neutral particle interactions) [2]. Plasma frequency, determined by electron density, dictates whether EM waves are reflected (below plasma frequency) or penetrate the ionosphere (above plasma frequency) [2]. The Finite-Difference Time-Domain (FDTD) method [3] is a computational technique for solving Maxwell's equations to model EM wave propagation and dispersion. By discretizing space and time into grids, FDTD iteratively calculates electric and magnetic field evolution, making it ideal for simulating complex geometries and time-dependent phenomena in plasma physics [3]. High-power microwave pulses can induce plasma turbulence in the ionosphere, altering wave propagation through refraction, scattering, and absorption. Such interactions degrade signal integrity, particularly in regions with plasma density irregularities [8]. This study examines the ionosphere's impact on ground-to-satellite communication signals, emphasizing its layered structure, plasma dynamics, and EM wave interactions. Insights into these phenomena are vital for optimizing wireless communication systems and mitigating ionospheric disruptions.

## II. THERSITICAL BACKGROUND

### a. Propagation in Ionosphere

The propagation of radio waves through the Earth's ionosphere involves the transmission of electromagnetic signals from the upper atmosphere. This process is highly complex due to the ionosphere's non-uniform structure, which consists of spatially and temporally varying densities of charged particles (free ions and electrons). These particles interact with radio waves, causing refraction, absorption, and scattering, which significantly influence signal behavior [9][10].

The propagation of electromagnetic pulses in the ionosphere can be modeled using Maxwell's equations adapted for cold, collisionless plasma. The governing equations are:

$$\frac{\partial J_P(r,t)}{\partial t} = \varepsilon_0 w_p^2 E(r,t) \qquad (1)$$

$$\varepsilon_0 \frac{\partial_E(r,t)}{\partial t} = \nabla X H(r,t) - J_P(r,t) \qquad (2)$$

$$\mu_0 \frac{\partial_H(r,t)}{\partial t} = \nabla X E(r,t) J_P \qquad (3)$$

In the equation =, E is electric intensity, H is magnetic intensity, $\mathrm{J_P}$ IS Polarization current density, $\mathrm{W_P} = \sqrt{\mathrm{n_e e^2/mc_0}}$ is angular frequency of plasma,[11].

### b. Effective Collision Frequency

The collision frequency affecting signals in the ionosphere varies with altitude due to interactions between electron density and collision frequency, which govern signal reflection and absorption. Repeated collisions between neutral particles and electrons dissipate wave energy as heat. In the lower ionospheric layers (D and E regions), collision frequency with neutral particles is significantly higher, causing pronounced absorption of low-frequency signals. In contrast, the F layer exhibits reduced collision frequency owing to the decreasing atmospheric density at higher altitudes. Consequently, signal absorption is most substantial in the D layer during daylight hours, whereas diminished absorption in the F layer enables efficient signal reflection, facilitating long-distance radio communication through the ionosphere [12]. During daytime, the D layer's presence strongly absorbs lower-frequency signals, while the F layer's elevated electron density reflects higher frequencies with minimal attenuation. At nighttime, the D layer dissipates, drastically reducing absorption. This allows lower-frequency signals to reflect off the E and F layers, extending their propagation range [14]. The high collision frequency in the D layer reduces the refractive index (as described by the Appleton-Hartree equation), promoting evanescent wave decay and energy absorption. Conversely, the F layer's lower collision frequency and higher electron density favor wave reflection with reduced energy loss [15]. Collision frequency in ionospheric plasma is fundamentally determined by interactions between free electrons, neutral molecules, and ions [16].

$$\mathrm{v = N.\sigma.\sqrt{\frac{8k_B T}{\pi m_e}}} \qquad (4)$$

N=Neutral particle density, σ =collisional cross-section, $k_B$ =Boltzmann constant, T =Kinetic temperature, $m_e$ =Electron mass.

**c. Transmission coefficient**

The transmission coefficient in the ionosphere determines the proportion of electromagnetic wave energy that penetrates the ionospheric layer, as this coefficient is inherently dependent on the wave's frequency of the wave ($\omega$ $or$ $f$) the frequency of the plasma ($\omega_p$) the collision frequency ($v$),**Angle of incidence**,[17].

a. Frequency bands and transmission

- Daytime:
  - Reflected by F-layer($f < f_c$) → $T \approx 0$
  - String D-layer absorption → low transmission.
- Nighttime:
  - D- D-layer vanishes→ reduced absorption .
  - Partial transmission if $f > f_c$(E/F lyres).

b. VHF/UHF(30MHz-3GHz)

- Typicality $f > f_c$ → penetrates ionosphere(T≈ 1).

c. LF/MF(30kHz-3MHz)

- Strong absorbed in D-layer($T \approx 0$)during daytime
- Nighttime reflects off E-layer($T > 0$).

**d. Electron density**

Electron density in the ionosphere governs electromagnetic wave propagation and exhibits variations with altitude, time, and geographic location. It ranges from approximately $10^3$ electrons per cubic meter ($e^-/m^3$) in the D-region to $10^{12}$ $e^-/m^3$ in the F-region. This density peaks at noon due to solar ionization and reaches its minimum at night as a result of ion-electron recombination processes [18].The refractive index of the ionosphere, which dictates the curvature of radio waves, is directly proportional to electron density. This relationship causes radio waves to bend and reflect back to Earth, resulting in phenomena such as radio wave fading, multipath interference, and scintillation [19]. The electron density in the ionosphere can be calculated using the following expression:

$$n_e = \frac{N_e}{V} \qquad (5)$$

Where:$n_e$ is the electron density in electrons per cubic meter (e/m^3), $N_e$ is the total electron content (TEC) in electrons per square meter (e/m^2), V is the volume integral of height in cubic electrons (m^3) of the ionosphere under consideration.

Electron density is commonly expressed in terms of physical parameters of the plasma:

$$n_e = \frac{\omega_p^2 \varepsilon_0 m_e}{e^2} \qquad (6)$$

$n_e$ =Electron density (m^-3),$\omega_p$ =Plasma frequency (rad/s), $\varepsilon_0$Permittivity of free space (8.85×10^-12 F/m). $m_e$= Electron mass (9.11×10^-31 kg), e = Electron charge (1.60×10^-19 C).

## III. METHADOLOGY

To analyze the ionosphere's impact on signal propagation, numerical simulations were conducted using the finite-difference time-domain (FDTD) method. This approach solves Maxwell's equations for electromagnetic (EM) wave propagation in a cold, collisional plasma, as modeled by the governing equations (Eqs. 1–3). The ionospheric medium was discretized into a spatial grid spanning altitudes from 50 km to 400 km, enabling iterative computation of the time-dependent evolution of electric (E) and magnetic (H) fields. The ionosphere comprises distinct layers (F, E, and D), each characterized by altitude-dependent parameters: electron density ($n_e$), plasma frequency ($\omega_p$), and effective collision frequency ($v$).. The plasma frequency ($\omega_p$), which governs the cutoff frequency for wave penetration, is calculated as:

$$\omega_p = \sqrt{n_e e^2 / m_e \varepsilon_0} \qquad (7)$$

$n_e$=Electron density, $m_e$ =Electron mass, $e$ = Electron charge, $\varepsilon_0$= Permittivity of free space.

The effective collision frequency (v)was derived from Equation (4), incorporating the neutral particle density (N), collision cross-section(σ) and temperature. These parameters were evaluated to quantify energy loss arising from collisions between free electrons and neutral particles. The transmission coefficient was determined using the Appleton-Hartree equation, which depends on the wave frequency (ω), plasma frequency ($\omega_p$), collision frequency (v), and angle of incidence. Simulations were conducted over a 24-hour cycle to capture diurnal variations, including daytime D-layer absorption and nighttime E/F-layer reflection effects. Total Electron Content (TEC) was calculated using GPS signal delays measured at dual frequencies (L1:1575.42 MHz, L2:1227.60 MHz), enabling correlation of ionospheric electron density with temporal variations. Group delay and frequency-dependent effects were computed from these dual-frequency measurements to quantify signal dispersion and absorption losses. Transmission coefficient vs. frequency, Collision frequency vs. altitude, TEC vs. time, Group delay and frequency effects.

## IV. EXPERIMENTAL RESULTS AND DISCUSSION

Fig. 1. illustrates the relationship between the ionospheric transmission coefficient and radio signal frequency for signals propagating through the ionosphere at altitudes of 50–400 km. As frequency increases, the transmission coefficient rises, attenuation diminishes, and the ionosphere becomes increasingly transparent. This enhanced transparency facilitates effective signal penetration. Conversely, at lower frequencies, penetration becomes less efficient due to heightened attenuation and a corresponding reduction in the transmission coefficient.

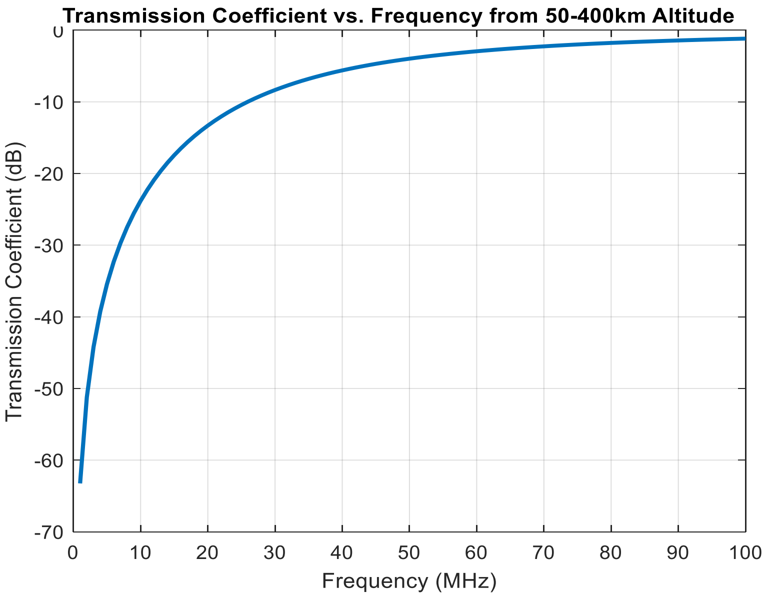


**Figure 1:** Transmission coefficient for the ionosphere from 50 km to 400 km

Fig. 2. (a) The plasma frequency ($\omega_p$), as a function of altitude exhibits a distinct peak, labeled as "Peak Density," corresponding to the F2-layer maximum. This curve demonstrates an initial increase in plasma frequency with altitude, followed by a gradual decline at higher altitudes. (b) The transmission coefficient is plotted against altitude and frequency, illustrating signal transmission efficiency across the ionosphere at varying heights and frequencies. A gradient color scale (blue to red) corresponds to variations in the transmission coefficient, with red indicating higher transmission efficiency and blue representing lower values.

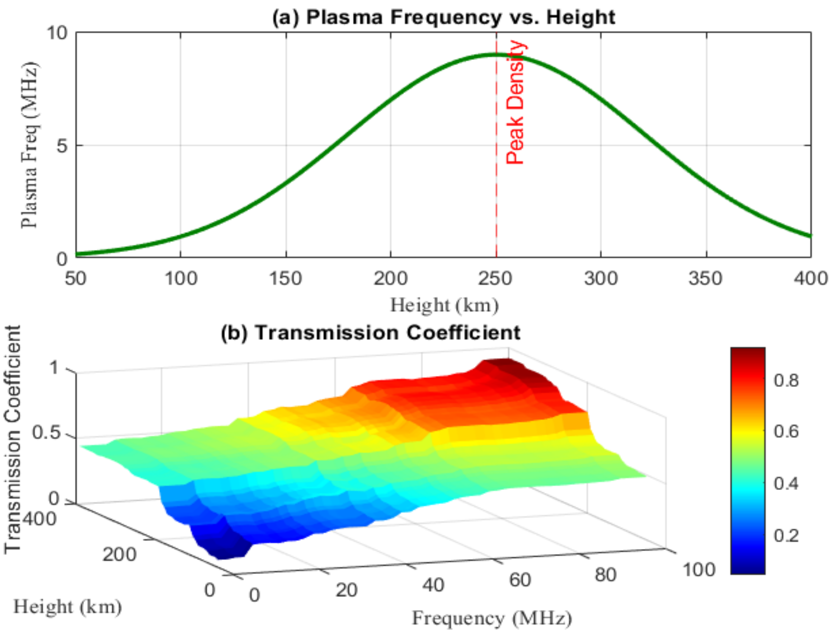


**Figure 2:** Variation of Plasma Frequency and Transmission Coefficient with Altitude in the Ionosphere.

Fig. 3. illustrates the relationship between effective collision frequency (ν) and altitude in the Earth's atmosphere. The curve demonstrates a decline in collision frequency with increasing altitude, attributable to the reduced gas density at higher elevations. In lower atmospheric layers (e.g., the D-region), higher gas density enhances the probability of molecular collisions. Conversely, in upper layers (e.g., the F-region), collisions diminish due to the sparser distribution of particles. When radio signals propagate through the ionosphere, they interact with charged particles (ions and electrons). The collision frequency directly influences signal dispersion and absorption: higher collision rates in dense lower layers exacerbate energy loss through absorption, while reduced collisions at higher altitudes permit more efficient signal transmission. The ionosphere, a region of Earth's upper atmosphere ionized by solar radiation, comprises free electrons and ions. Radio waves traversing this layer undergo scattering and attenuation due to interactions with these charged particles, with collision frequency serving as a critical parameter governing signal behavior.

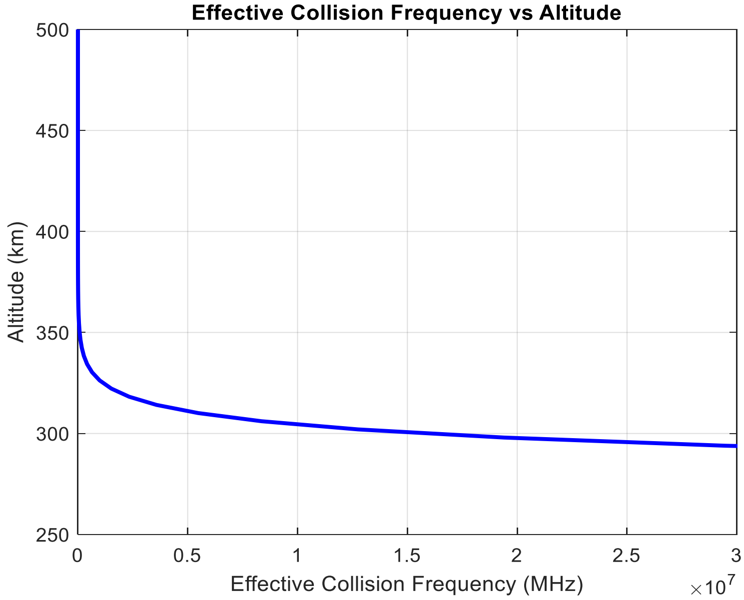


**Figure 3:** Effective collision frequency.

Fig. 4. illustrates the diurnal variation of Total Electron Content (TEC) over a 24-hour period. TEC quantifies the integrated number of free electrons in a vertical column of the ionosphere. The plot reveals a distinct daily cycle: TEC begins at a minimum value during early morning hours (approximately 01:00), gradually increases to a peak near local noon (12:00), and subsequently declines to a nighttime minimum by 24. This pattern reflects the ionosphere's response to solar radiation. During daylight hours, solar ultraviolet and X-ray radiation ionize atmospheric gases, elevating electron density. At night, in the absence of sunlight, ion-electron recombination dominates, reducing TEC. Such diurnal behavior underscores the critical role of solar activity in modulating ionospheric plasma density and its subsequent effects on radio wave propagation.

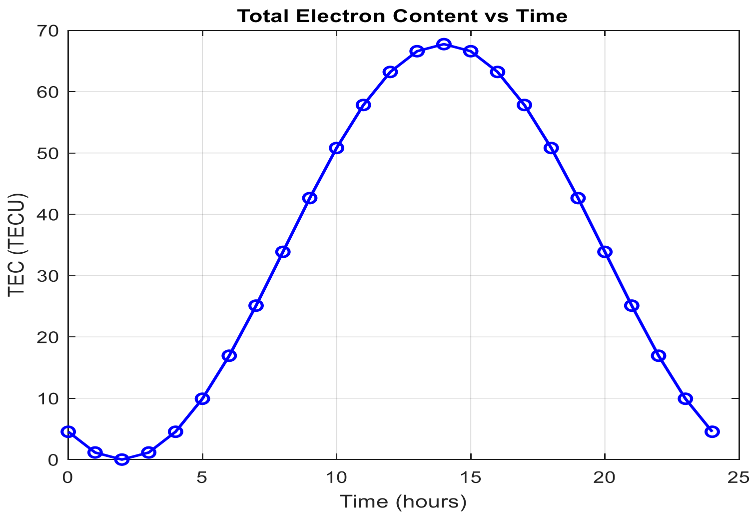


**Figure 4:** Relationship between total electron content (TEC) and vs Time.

Fig. 5. presents a three-dimensional visualization of ionospheric electron density ( $\times 10^{11}$ $m^{-3}$) as a function of altitude (50–400 km) and local time. The diurnal cycle reveals peak electron density during midday (12:00–18:00 ), driven by solar ionizing radiation. The maximum density ($10^{11}$ $m^{-3}$) occurs near 250 km altitude, corresponding to the F-layer, and declines sharply above 300 km due to reduced atmospheric density. The model successfully reproduces the characteristic day-night asymmetry in electron density, a critical feature for understanding radio signal propagation.

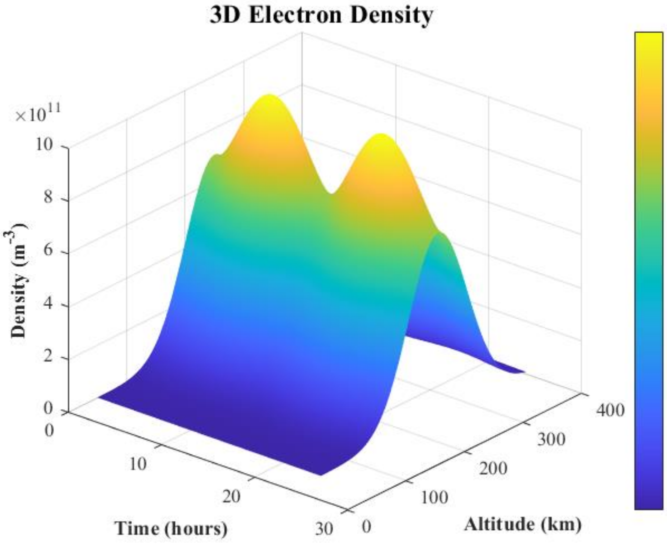


**Figure 5:** shows Diurnal Variation of Electron Density in the Ionosphere with Altitude.

Fig. 6. depicts the relationship between group delay and time for dual-frequency GPS signals (L1: 1575.42 MHz, L2: 1227.60 MHz) over a 24-hour period. The horizontal axis represents local time (hours), while the vertical axis quantifies group delay in nanoseconds (ns). Both signals follow a diurnal pattern: group delay increases to a maximum near midday and subsequently decreases, forming a quasi-sinusoidal trend. The observed asymmetry in group delay magnitude between L1 and L2 reflects differences in ionospheric dispersion characteristics, which arise from frequency-dependent interactions with free electrons in the ionosphere. The bell-shaped curves suggest a correlation with Total Electron Content (TEC), which peaks during daylight hours due to solar ionization. Environmental factors such as ionospheric electron density gradients and geomagnetic activity likely contribute to the temporal variations in signal propagation.

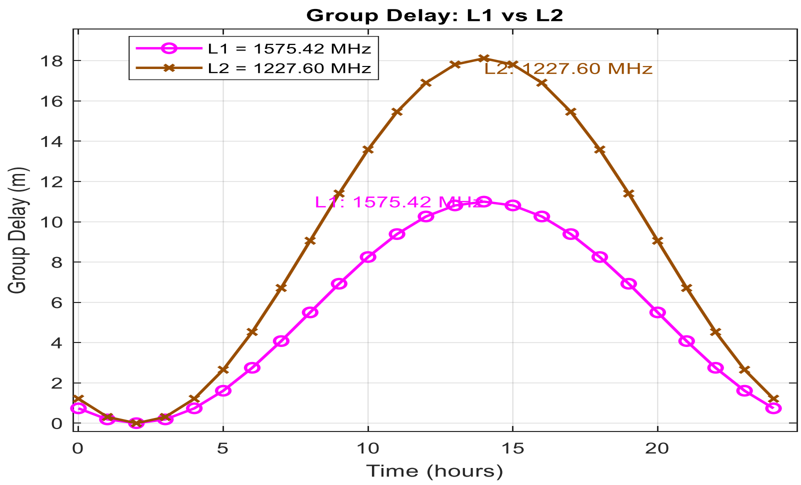


**Figure 6:** Relationship between group delay (Group Delay) and Time.

Fig. 7. illustrates the diurnal variation of the frequency-dependent ionospheric effect (dB) over 24 hours. The vertical axis quantifies the frequency effect, defined as the differential attenuation between the L1 (1575.42 MHz) and L2 (1227.60 MHz) GPS signals, while the horizontal axis represents time in hours. The data exhibits a distinct diurnal pattern: the frequency effect begins at a maximum during early morning hours (01:00), decreases to a minimum near midday (12:00–14:00), and gradually increases again toward nighttime (24:00). This periodic

behavior reflects ionospheric modulation by solar radiation. During daylight hours, enhanced solar ionization elevates electron density, reducing the differential attenuation between L1 and L2. At night, diminished ionization amplifies the frequency-dependent disparity, consistent with ionospheric recombination processes. The observed trend underscores the influence of Total Electron Content (TEC) dynamics on signal propagation. Reduced midday attenuation aligns with peak TEC values, enabling more uniform signal dispersion across frequencies, while nighttime conditions exacerbate frequency-selective fading.

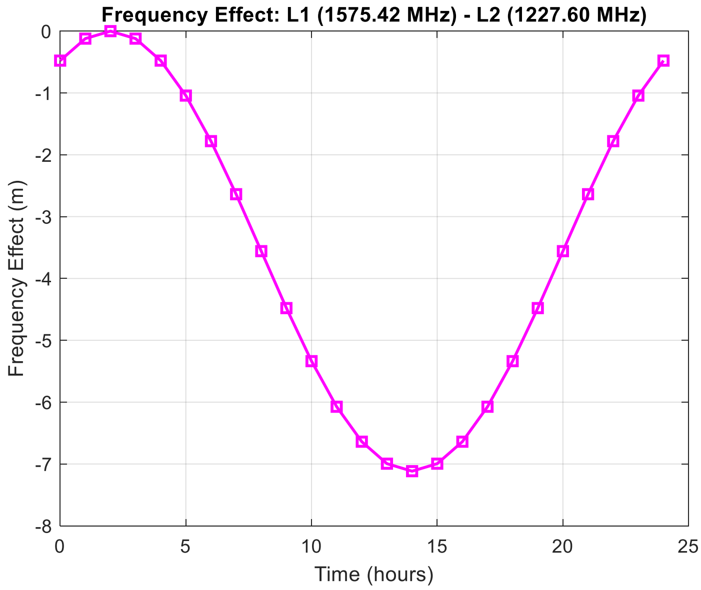


**Figure 7:** Relationship between Frequency Effect vs Time.

Fig.8. depicts diurnal variations in ionospheric electron density profiles across altitudes (50–400 km) at four local times: 06:00, 12:00, 18:00, and 24:00. The vertical axis represents altitude (km), while the horizontal axis quantifies electron density (units: $10^{11}$ $cm^{-3}$). Each curve characterizes altitude-dependent electron density variations at distinct times. The density peaks in the F-layer (250–300 km altitude) and declines sharply above 300 km due to reduced atmospheric particle density. The profiles exhibit significant temporal variability: Daytime (12:00): Maximum electron density (~$10^{11}$ $cm^{-3}$) driven by solar ionization. Nighttime (24:00): Reduced density (~$10^{10}$ $cm^{-3}$) due to ion-electron recombination. The observed diurnal asymmetry in profile shapes reflects dynamic ionospheric processes, including solar zenith angle variations and geomagnetic activity. These variations influence radio wave propagation, with daytime profiles favoring signal reflection and nighttime conditions increasing absorption.

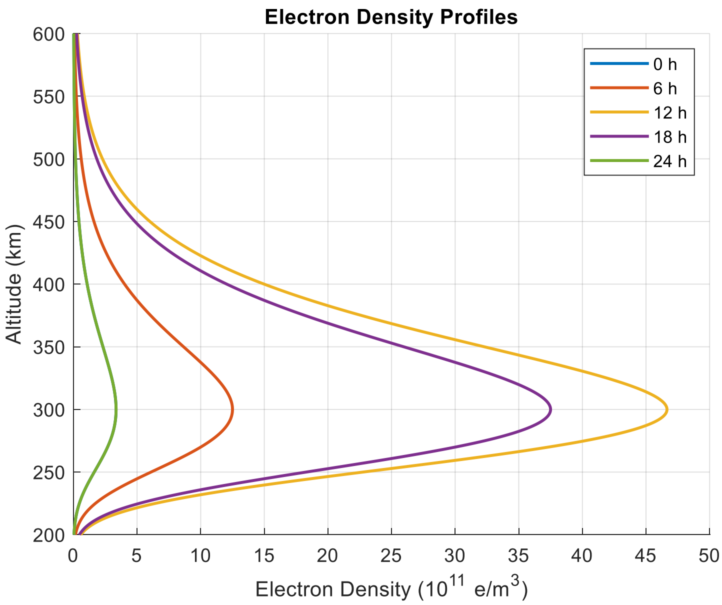


**Figure 8:** Relationship between electron density (10^11/cm^3) and Altitude(km).

**Table 1:** Diurnal Variation of Total Electron Content (TEC), GPS Group Delays (L1/L2), and Frequency Effect in the F-layer.

| Time-h | TEC_TECU | GroupDelay1_m | GroupDelay2_m | Frequency Effect_m |
|---|---|---|---|---|
| 1 | 4.5382 | 0.73687 | 1.2136 | -0.47672 |
| 2 | 1.1542 | 0.18741 | 0.30866 | -0.12124 |
| 3 | 1.1542 | 0.18741 | 0.30866 | -0.12124 |
| 4 | 4.5382 | 0.73687 | 1.2136 | -0.47672 |
| 5 | 9.9213 | 1.6109 | 2.6531 | -1.0422 |
| 6 | 16.937 | 2.7501 | 4.5292 | -1.7791 |
| 7 | 25.106 | 4.0766 | 6.7139 | -2.6373 |
| 8 | 33.873 | 5.5001 | 9.0584 | -3.5583 |
| 9 | 42.64 | 6.9236 | 11.403 | -4.4792 |
| 10 | 50.81 | 8.2502 | 13.588 | -5.3374 |
| 11 | 57.825 | 9.3893 | 15.464 | -6.0743 |
| 12 | 63.209 | 10.263 | 16.903 | -6.6398 |
| 13 | 66.593 | 10.813 | 17.808 | -6.9953 |
| 14 | 67.747 | 0.011 | 18.117 | -7.1165 |
| 15 | 66.593 | 10.813 | 17.808 | -6.9953 |
| 16 | 63.209 | 10.263 | 16.903 | -6.6398 |
| 17 | 57.825 | 9.3893 | 15.464 | -6.0743 |
| 18 | 50.81 | 8.2502 | 13.588 | -5.3374 |
| 19 | 42.64 | 6.9236 | 11.403 | -4.4792 |
| 20 | 33.873 | 5.5001 | 9.0584 | -3.5583 |
| 21 | 25.106 | 4.0766 | 6.7139 | -2.6373 |
| 22 | 16.937 | 2.7501 | 4.5292 | -1.7791 |
| 23 | 9.9213 | 1.6109 | 2.6531 | -1.0422 |
| 24 | 4.5382 | 0.73687 | 1.2136 | -0.47672 |

The data highlights diurnal trends in ionospheric conditions, such as elevated TEC and reduced group delays during midday due to solar ionization, and increased frequency effects at night caused by ionospheric recombination. These variations correlate with fluctuations in GPS positioning accuracy, as ionospheric disturbances induce signal path delays and phase distortions**.**

## V. CONCLUSION

This study examines the ionosphere's plasma layer effects on Earth-satellite signal propagation by analyzing plasma frequency, effective collision frequency, and Total Electron Content (TEC). Results demonstrate that signal transmission through the ionosphere is highly frequency-dependent: higher frequencies exhibit greater transmission coefficients due to reduced ionized particle interactions, enabling effective penetration, while lower frequencies suffer severe attenuation, particularly in the daytime D-layer. Effective collision frequency, governing energy loss from electron-neutral collisions, decreases exponentially with altitude due to declining atmospheric density, minimizing absorption in the F-layer. Diurnal TEC variations peak during daylight hours under solar radiation and decline nocturnally due to recombination, directly modulating electron density and propagation characteristics. Group delay and collision frequency correlate temporally with TEC maxima, underscoring the ionosphere's role in signal degradation via absorption, dispersion, and scintillation. To improve communication reliability, systems must account for altitude-dependent collision rates, diurnal electron density shifts, and frequency-specific ionospheric interactions. Future work should prioritize real-time TEC monitoring, refined collision models, and adaptive modulation techniques to mitigate disruptions caused by solar activity variations.

## References


[1] Köhn, Alf, et al. "Influence of plasma turbulence on microwave propagation." Plasma Physics and Controlled Fusion 58.10 (2016): 105008.V. L. Ginzburg, The Propagation of Electromagnetic Waves in Plasmas, 2nd ed. New York, NY: Pergamon Press, 1970.

[2] Chen, Francis. Introduction to plasma physics and controlled fusion. Springer, 2015.

[3] Kweon, Jun-Ho, et al. "FDTD analysis of electromagnetic wave propagation in an inhomogeneous ionosphere under arbitrary-direction geomagnetic field." Journal of Electromagnetic Engineering and Science 18.3 (2018): 212-214.

[4] Davies, Kenneth, and Ernest K. Smith. "Ionospheric effects on satellite land mobile systems." IEEE Antennas and Propagation Magazine 44.6 (2002): 24-31.

[5] Liu, Tao, et al. "Influence of the Ionosphere E Layer on the Capacity of Satellite-to-Ground Quantum Communication Channels." 2022 IEEE 10th International Conference on Information, Communication and Networks (ICICN). IEEE, 2022.
[6] Molina, Carlos, and Adriano Camps. "First evidences of ionospheric plasma depletions observations using GNSS-R data from CYGNSS." Remote Sensing 12.22 (2020): 3782.
[7] Petrin, Andrei B. "Transmission of microwaves through magnetoactive plasma." IEEE transactions on plasma science 29.3 (2001): 471-478.
[8] Armand, N. A., et al. "Radiowave propagation through a turbulent plasma disturbed with radio irradiation." (1985).
[9] Blagoveshchensky, D. V., et al. "Modeling of HF propagation at high latitudes on the basis of IRI." Advances in Space Research 57.3 (2016): 821-834.
[10] Yang, Dan, Hai-jun Fu, and Cheng Liao. "Investigations of microwave pulse propagation in ionosphere." 2010 Asia-Pacific International Symposium on Electromagnetic Compatibility. IEEE, 2010.
[11] Yang, Dan, Cheng Liao, and Wei Chen. "The Study of High Power Microwave Pulse Propagation in the Ionosphere." 2006 7th International Symposium on Antennas, Propagation & EM Theory. IEEE, 2006.
[12] Kelley, Michael C. The Earth's ionosphere: Plasma physics and electrodynamics. Vol. 96. Academic press, 2009.
[13] Zawdie, Kate A., et al. "Calculating the absorption of HF radio waves in the ionosphere." Radio Science 52.6 (2017): 767-783.
[14] Kuverova, V. V., et al. "Chemical physics of D and E layers of the ionosphere." Advances in Space Research 64.10 (2019): 1876-1886.
[15] Haider, S. A., et al. "Zonal wave structures in the nighttime tropospheric density and temperature and in the D region ionosphere over Mars: Modeling and observations." Journal of Geophysical Research: Space Physics 114.A12 (2009).
[16] Huba, Joseph D., Robert W. Schunk, and Georgiĭ Vladimirovich Khazanov, eds. Modeling the ionosphere-thermosphere. John Wiley & Sons, 2014.
[17] Budden, Kenneth George. The propagation of radio waves: The theory of radio waves of low power in the ionosphere and magnetosphere. Cambridge University Press, 1988.
[18] Kuo, Spencer P., and Angqing Ren. "Experimental study of wave propagation through a rapidly created plasma." IEEE transactions on plasma science 21.1 (1993): 53-56.
[19] Petrin, Andrei B. "Transmission of microwaves through magnetoactive plasma." IEEE transactions on plasma science 29.3 (2001): 471-478.